Fast-and-easy acoustic optimization of PMSM by means of hybrid modeling and FEM-to-measurement transfer functions

M. van der Giet, D. Franck, R. Rothe and K. Hameyer

***Abstract*—This paper proposes a methodology for the acoustic optimization of PMSM applying two steps: hybrid modeling to obtain the magnetic field and forces at comparatively small computational effort and FEM-to-measurement transfer functions to assess the structural behavior and the radiation characteristics of the machine at once. Both steps are explained and applied to a specific PMSM design, which is subject to optimization. The proposed approach relies on a (virtual) protoype. The resulting optimized geometry shows significant reduction potential in terms of total sound pressure level, up to 18dB(A), but at the cost of a larger magnet volume. Limitations of this procedure are discussed.**

***Index Terms*—Acoustic optimization, audible noise, noise and vibration, PM synchronous machine, variable speed drive**

I. Introduction

Nowadays, radiated audible noise is becoming more and more relevant in many applications. Permanent-magnet excited synchronous machines (PMSM) are employed in many cases as variable speed drive because of their high power density and efficiency. The increase of power density typically goes together with an increase of air-gap flux-density level, leading to higher electromagnetic force excitation and ultimately to higher audible noise radiated by the machine.

Therefore, this paper proposes a methodology to optimize the acoustic performance of a PMSM drive in terms of electromagnetic excitations. The objective is to minimize the maximum sound pressure level (SPL) in dB(A) due to electromagnetic force excitations during the complete run-up of the machine with no mechanical load. It is shown how microphone measurement of a given (virtual) prototype for the target application and numerical field calculation of the PM together with an analytical description of the stator slotting can be exploited to optimize the acoustic behavior of a variable speed PMSM. Virtual prototype refers here to the numerical simulation model in terms of structural dynamics and acoustic radiation, which has been validated for machines using the same manufacturing technology and having a similar size. The application of the proposed approach is limited here to the no-load case, because the studied device already showed high acoustic emission in this operation. Due to the minor influence of the stator slot geometry for distributed windings, the permanent magnet (PM) shape is considered to be the only optimization parameter. In principle however, the approach may be extended to optimize for full-load operation and include the stator slot geometry if needed.

All authors are with the Institute of Electrical Machines - RWTH Aachen University, Germany phone: +49 241 80 97636, e-mail: mvdg@iem.rwth-aachen.de

Acoustic noise of electrical machines is known and troublesome since many years. An early hint is given by Fischer-Hinnen [1], who describes the “howling” and “whistling” of electrical machines as unpleasantness, which may even lead to drawing back such machines after delivering.

The audible noise from rotating electric machinery is typically classified according to their origin. It can be distinguished between noise due to the electromagnetic field, due to pure mechanical reasons, i.e. bearing, and due to aerodynamic phenomena, i.e. fan blades of air-cooled machines. This division was already introduced by Frohne in 1959 [2]. Audible noise in rotating machines, stemming from electromagnetics can further be subdivided into the following excitation categories: reluctance forces, Lorentz forces, magnetostriction and magneto-mechanical coupling [3].

Though the emitted noise of electrical machinery has more sources than the electromagnetic forces, the majority of research has been done on the electromagnetically excited noise, due to its predominant role. This is due to the fact that the electromagnetic noise is different from most other noise phenomena, which mostly stem from mechanical origin. In addition, the electromagnetic noise, due to the periodicity of the fields and forces typically generate single tones, which unfortunately often lay within a frequency band, in which the human ear is most sensitive [4].

During the first half of the 20th century, Jordan introduced the idea that the interaction of electromagnetic force density waves with the mechanical and acoustic characteristics of the machine is the key to understanding and solving the problem of audible noise of electric machinery. In [4], Jordan uses the rotating field theory and derives formulas for the occurring ordinal numbers of the rotating field waves, calculates the eigenfrequencies and forced vibration of stators, treated as thin rings and even approximates the radiated acoustic power level of induction machines.

The numerical simulation of electromagnetic force excitations and of forced vibration as the outcome of structural simulation together presents a so called coupled problem.An early reference to address forced vibration of electrical machines is dated to 1992 by Henneberger et al., who use 2D finite-element method (FEM) numerically weak-coupled between electromagnetics an structural dynamics to compute vibration of synchronous alternators [5]. At the end of the 1990ies, coupling electromagnetic and structural FEM in addition to an acoustic boundary element method (BEM) simulation became standard procedure [6], [7], [8].

The influence of the PM shape on the electromagnetic force excitation and on the vibrational behavior of PMSM has been analyzed [9], e.g. radially magnetized magnets showed a fre-

quency spectrum of force excitations with higher components at higher frequencies, due to the block shaped B-field. Block shaped magnets have a higher fundamental component and significantly less higher harmonics. Particularly in the case of tooth coil windings, the significance of the pole shape has been pointed out and exploited to optimize the vibrational behavior in the sense of torsional vibrations, i.e. reduction of cogging torque, [10]. For tooth-coil windings, a partly enlarged air gap has been proposed as a measure for improving the acoustic behavior of PMSM [11]. In [12], the shape of interior PMs is optimized towards the minimum torque ripple. In addition to that, mechanical vibration due to electromagnetic excitations are minimized in [13].

The influence of geometrical parameters of stator and rotor on the acoustic performance on a PMSM drive is investigated in [14], design-of-experiment methodology is employed to keep the number of necessary numerical simulations low. In contrast to this paper, the vibrational and acoustic behavior is assessed individually by means of a vibrational measurement (modal analyses) and an analytical radiation model. Vivier et al. use an analytical model for the magnetic circuit parameters and do not account for complicated magnet geometry.

The idea of FEM-to-measurement transfer function can also be found in [15]. In his thesis, Roivainen analyses the vibro-acoustic behavior of direct-torque-controlled (DTC) induction machines. Therefore, a structural dynamic analysis using unit-forces is performed. For verification purposes, the surface acceleration of the machine is measured and the unit-force transfer function is defined as the ratio of measured acceleration to simulated forces. Sound pressure measurement are not used for the measurement-to-FEM transfer functions.

Compared to the approaches presented in the literature, in this paper two novel aspects are presented, one is the usage of hybrid-analytical-FEM modeling, the second one is the usage of microphone measurements for FEM-to-measurement transfer functions for the acoustic optimization of PMSM. The latter one may not be as accurate as measuring solely the mechanical transfer function as e.g. in [15], but may be sufficient for optimization starting from an existing prototype, which may have poor acoustic performance, and it is easy in terms of measurement. Furthermore, no sufficient acoustic model, structural and radiation, model is needed.

The outline of the remaining text of this paper reads as follows: First the methodology of FEM-to-measurement transfer functions on the one hand and the hybrid modeling approach on the other hand are explained. Secondly, the approach is applied to the optimization of PM shape of a variable speed inverter fed PM synchronous motor, of which the optimal design is presented, compared to the reference design and verified by full model 2D FEM simulations. A summary and discussion concludes the paper.

II. Method

A. Reduction of force excitation level

As a first step in the development of this work, the authors analyzed the acoustic radiation of the studied PMSM. Comparison with table of ordinal numbers that occur in synchronous machines revealed those harmonic force waves that were exciting the mechanical structure and thus leading to disturbing audible noise during the run-up of the PMSM [4]. Tracing the relevant force waves back to their originating flux density waves, the PM shape has been altered in such a way that the specific harmonic in the air gap field is almost canceled out. However, this approach has not yielded completely satisfactory results in a cases, for three reasons: First this simplified approach, does not account for structure and radiation of the machine. Second, it does not take the run-up into consideration and finally the interaction of PM and stator slotting is neglected in this approach. The first two issues are coped with by means of the FEM-to-measurement transfer function. In The second and third aspect are described using the hybrid modeling.

B. FEM-to-measurement transfer functions

Electromagnetically excited audible noise from electrical machines is typically analyzed in three simulation steps: 1) Electromagnetic field and forces, 2) Mechanical oscillating deformation, and 3) acoustic radiation and perception [4]. Each step can be either investigated by analytical calculation, by numerical simulation or by measurement. In this sense, there is a signal (and energy) flow from current/PM excitation, via flux density and reluctance forces, through surface velocity to sound pressure and particle velocity. For each of the three parts a transfer function can be defined, where the transfer function of the latter two typically can be considered being linear. For example, the mechanical transfer function can be determined by means of numerical modal analysis (using FEM) or by means of experimental modal analyses (using shaker, accelerometer and dual-spectrum analyzer), for a point excitation.

Alternatively to defining the transfer function purely from measurement, or purely from simulation, it is possible to define a mixed form, if it can be assured that the operating conditions are approximately equal, in the sense

$$H = \frac{B_{meas}}{A_{simu}}\,, \tag{1}$$

where B_{meas} is the measured output of the transfer function, and A_{simul} is the simulated input. Using magnetic forces as A_{simu} is a good choice for two reasons: First they can be simulated comparatively accurate using 2D-FEM and they are very difficult to measure. In [15], B_{meas} is chosen to be the surface acceleration and A_{simu} is indeed the magnetic force. In this paper, the transfer function of 2) and 3) is considered at once, thus the sound pressure is used as B_{meas} .

The starting point for the determination of transfer functions is a microphone measurement of sound pressure $p_{meas}(t)$ and a synchronized speed measurement $n(t)$ during a unloaded run-up of the PMSM with sufficiently slow slew rate. This is mapped to a so called waterfall diagram given by $p_{meas}(\omega, 2\pi n)$, which shows dominant lines due to harmonic force excitations, see Fig. 3. Using a peak-picking technique along these lines, allows for the definition of lines of constant order k as $p_{meas}(\omega, k)$, $k = \frac{\omega}{2\pi n}$, which can be seen form Fig. 4.

As a second step, it is essential to trace back each order line to a specific harmonic. This can either be done using standard table works [4], or more sophisticated even tracing back to individual field harmonics [16], the latter detailed approach is not necessary for the method proposed in this paper, it however

may reveal more insight and may help trouble shooting the computer routines. For the unloaded run-up, the space vector diagrams are flat, i.e. there is no imaginary component of the force waves, due to the absence of stator currents. The Fourier decomposition of the reluctance-force-density waves reads

$$\sigma(x,t) = \sum_{k=1}^{K} \sum_{r=-R}^{R} \hat{\sigma}_{rk} \cos(rx + k \cdot 2\pi n \cdot t + \varphi)\,. \quad (2)$$

Now the assumption is made, that one harmonic force wave given by frequency harmonic number k' and by wave number r is dominant and solely accounted for at one line of constant order. Then, the FEM-to-measurement transfer function is defined as

$$H_r(\omega) = \frac{p_{meas}(\omega,k)}{\hat{\sigma}_{rk}}\Big|_{k=k'}\,, \quad (3)$$

where $\hat{\sigma}_{rk}$ is determined from a FEM simulation of the very geometry as the prototype delivering sound pressure measurements $p_{meas}(\omega,k)$.

The SPL for a given force excitation $\tilde{\sigma}_{rk}$ can be calculated by means of superposition:

$$L_p(\omega,n) = 20\log\left(\sum_{k=\frac{\omega}{2\pi n}}^{K} \sum_{r=-R}^{R} \frac{\tilde{\sigma}_{rk}\cdot H_r(\omega)}{p_{ref}}\right) - \Delta_A(\omega)\,, \quad (4)$$

where $p_{ref} = 2\cdot 10^{-5}\mathrm{N/m^2}$, however all results presented in this paper are referred to a slightly different undisclosed reference pressure leading to an undisclosed offset in all level plots.

To compensate for the frequency dependency of the human ear, measured or simulated audible signals are passed through a filter, of which the A filter is the most common. Therefore, (4) gives the unweighted pressure level in dB, if $\Delta_A(\omega) = 0, \forall\omega$ and it gives SPL in dB(A), if the A filter values are used for $\Delta_A(\omega)$.

The quadratic pressure levels of incoherent signals may be summed up immediately. Therefore, the (A-weighted) total SPL is then given by

$$L_{p,tot}(n) = 10\log\sum_{l=1}^{N} 10^{L_p(l\omega_0,n)/10} \quad (5)$$

in dB(A), where ω_0 corresponds to the window, which was initially used to determine $p_{meas}(\omega, 2\pi n)$. The next section is devoted to the question, how to calculate $\hat{\sigma}_{rk}$ efficiently for various PM shapes and speeds.

C. Hybrid modeling

The electromagnetic excited audible noise is generated by harmonics of the air-gap field. Therefore, simple methods taking only the fundamental air-gap flux density wave into account are prohibited and more detailed approaches are needed. Nowadays, numeric methods such as the FEM are usually applied. They are characterized by a high level of detail in the model, such as non linear material characteristics and exact description of the geometry, but they are computational expensive. Especially in conjunction with parameter variations or geometrical optimization the FEM leads to unacceptably large computational costs. The proposed hybrid model is accurate in terms of the significant properties, still leading to a reduction of the computational costs. In the presented study, the acoustic radiation in no-load condition is of major interest. Therefore, the influence of saturation is negligible. Hence, analytic methods such as the conformal mapping approach are suitable for the air-gap field computation [17]. In general the solution is obtained by solving a linear Laplace problem, described by the geometry. The magnetic permeability is assumed to be linear, which results in a linear time invariant system consequently. This allows for an individual modeling of the stator slotting, permanent magnet field and the field of the coils. In the first step the slotting is modeled by means of a complex relative permeance function [17] [18]

$$\underline{\lambda}\,(x) = \lambda^{rad}(x) + \jmath\lambda^{tan}(x). \quad (6)$$

where x denotes the angular position; $\lambda^{rad}(x)$ and $\lambda^{tan}(x)$ its radial and tangential component, respectively. In the next step the flux density of the permanent magnet is calculated considering a slot-less air gap. Since loaf shaped magnets are studied a separation of variables of the differential equation system is not possible, therefore a numerical solution is calculated. To reduce the computational effort, half a pole pitch is modeled by means of FEM and the radial and tangential air-gap flux density are gained by sampling. The entire field is reconstructed applying the symmetric properties of the machine and is described periodically on $x \in [0, 2\pi)$ by

$$\underline{B}_{pm}\,(x) = B_{pm}^{rad}(x) + \jmath B_{pm}^{tan}(x), \quad (7)$$

The air-gap flux density for one revolution of the rotor can be calculated by circular time-shift of (7) and multiplication with (6):

$$\underline{B}_{slot}\,(x,t) = \Re\left\{\underline{B}_{pm}(x - 2\pi n\cdot t)\cdot\underline{\lambda}^{*}\right\}, \quad (8)$$

In Fig. 1 the air-gap flux density obtained by the hybrid model and by a full FEM are compared. The air-gap field of one pole pair is presented. The important harmonics of the air-gap field obtained by the hybrid model are in good agreement with the FEM solution. The surface force density acting on the stator teeth is calculated by means of the simplified Maxwell stress tensor

$$\sigma\,(x,t) = -\frac{\left(\underline{B}_{slot}\,(x,t)\right)^2}{2\mu_0}, \quad (9)$$

where μ_0 is the magnetic permeability of vacuum. The force density waves are decomposed by a two dimensional Fourier transformation of (9), which yields (2). The flux density solution is calculated for one speed and the frequency and ordinal orders of the force density wave are used for the further investigation. The acceleration of the motor is considered in the total sound pressure calculation. With this approach the computational effort can be reduced from several hours to less then a minute for the simulation of one run-up, while the important aspects are modeled with a sufficient accuracy.

III. Results

A. Measurement basis

The studied and optimized PMSM is run up without additional inertia, but with a low slew rate (12.25 rpm/s). During the acceleration process, speed and sound pressure are

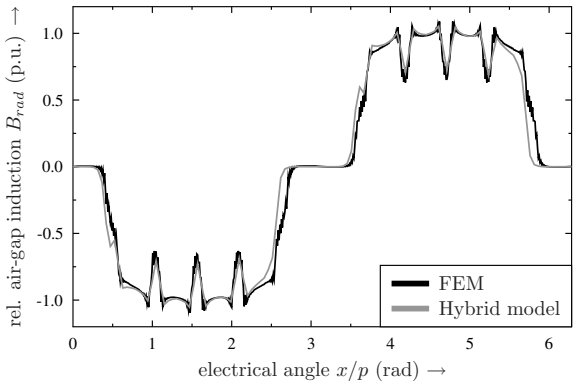

Figure 1. Comparison of air-gap flux-density: FEM and hybrid model.

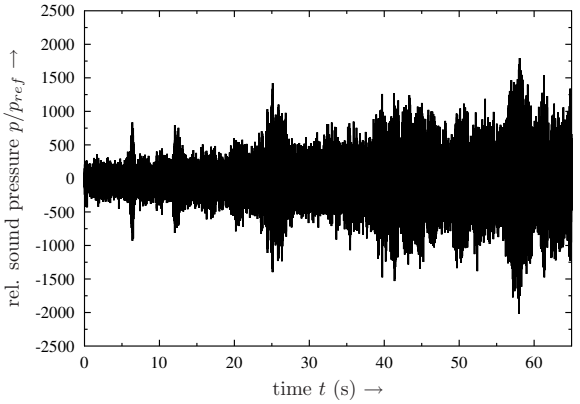

Figure 2. Microphone measurement of a PMSM run-up.

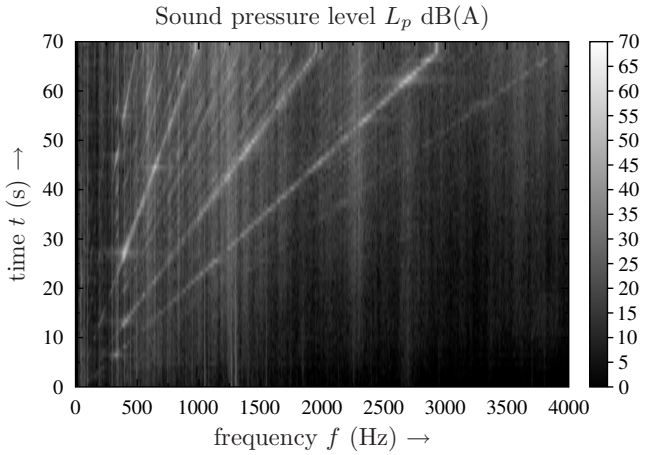

Figure 3. Waterfall diagram of the PMSM run-up.

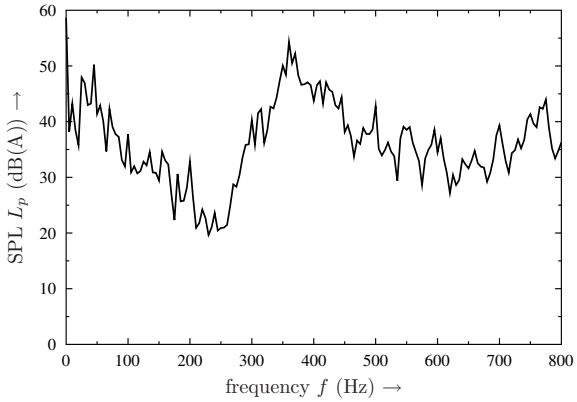

Figure 4. Sound pressure for constant order k.

measured synchronized to each other. As it be taken from the Fig. 2, the RMS value of the sound pressure increases with speed, though there are speeds, at which additional peaks occur. These peaks can be identified to be mechanical resonances of the PMSM structure.

Taking this data and applying a time limited discrete Fourier transform (DFT) of the acoustic pressure time history, it is possible to come to a so called waterfall representation, e.g. pressure as a function of time (this means speed in the linear run-up) and frequency. The window used for the DFT is in this case 200 ms. Fig. 3 shows the waterfall diagram derived from the microphone measurements. Straight lines are identified to be harmonic orders in the sound pressure and can be considered as constant time harmonic orders of displacement and also force excitation. Color is indicating the intensity at a specific point, resonances can be seen from very bright spots at a certain frequency and for all orders.

B. Derived transfer functions

From the waterfall representation, the sound pressure for constant order can be derived by collecting the sound pressure values along a constant order line. This representation is depicted in Fig. 4. Resonances, as well as the general increase with frequency are visible.

As described in section II-B, the sound pressure values for constant orders are referred to the FEM simulation of run-up. Owing to the fact, that it is a synchronous machine and eddy currents are disregarded, there is no need to perform a true transient electromagnetic FEM analysis. Instead, it is sufficient to compute one electrical period as quasi-static electromagnetic field problems. Fig. 5 depicts the transfer functions for mode numbers $r = 0, 4$ and 6. One limitation of this approach, which becomes visible, is the fact that transfer functions can be obtained only for those mode numbers that are present in the force density excitation spectrum. A further limitation is given by the available frequencies, up to which the transfer function is defined. This cut of frequency is given by the maximum speed during the run-up measurement and the order at which the mode number is excited.

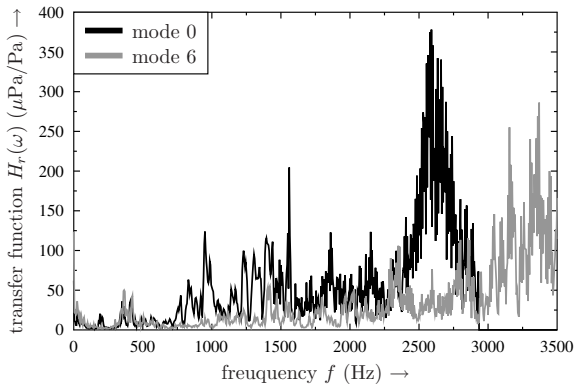

Figure 5. Derived FEM-measurement transfer functions.

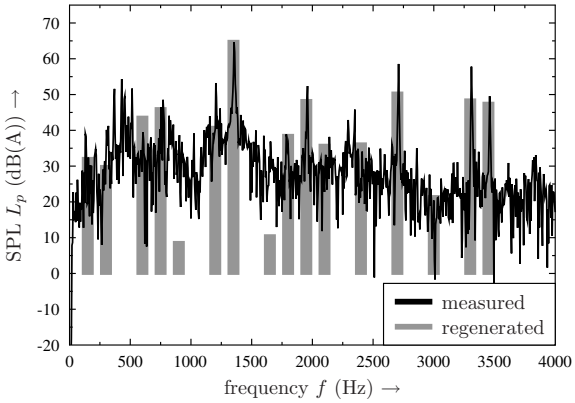

Figure 6. Comparison of measured and regenerated sound pressure.

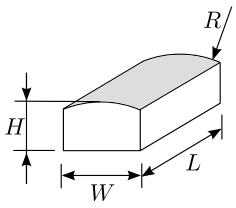

Figure 7. Geometrical definition of magnet shape [19].

As a check for the assumption, that only one excitation mode number is acting at a given frequency and order, the transfer function is multiplied with the FEM force densities and the outcome is compared to the measured sound pressure. From Fig. 6, it can be taken that all significant peaks in the sound pressure curve match reasonably well.

C. Result of the optimization

The PM shape is optimized starting from an undisclosed reference geometry. The geometry is defined by three parameters (H, W, L, R) shown in Fig. 7. Additionally, the mechanical air-gap δ is varied. The axial length of the magnets is equal to that of the active length of the machine and is kept constant. The objective of the optimization in this study is to reduce the maximum occurring total SPL during a run-up. Therefore, the objective function is defined as

$$f(H, W, R, \delta) = \max_n L_p \,.$$

The optimization problem is to find a combination (H, W, R, δ) that minimizes f under manufacturability boundary constrains. The flux density in the air gap was used as additional constraint (95% to 110%), in order to obtain a similar mean drive torque, which has to be verified after the optimal design is found. Since the computation time of the hybrid approach is very low, the four-dimensional parameter space is discretized between the min/max values and the objective function is computed for every combination (H, W, R, δ).

Table I gives a comparison between the reference design and the optimized design as well as minimum and maxim values. It can be seen that the maximum occurring total SPL is reduced by approx. 18 dB(A). This is done on the expense of more needed PM material, as the cross sectional area is 26% higher to keep the fundamental flux density though the air gap is increased by 17%.

Table I
COMPARISON OF REFERENCE AND OPTIMIZED GEOMETRY.

Quantity	Min	Max	Reference	Optimized
Magnet height H	83%	133%	100%	120%
Magnet width W	78%	117%	100%	111%
Magnet radius R	85%	115%	100%	84%
Air-gap length δ	83%	117%	100%	117%
Cross sectional area of PM			100%	126%
Magnet-pitch to pole-pitch			80%	88%
Fundamental flux density B	95%	110%	100%	101%
THD of air gap flux density			35%	11%
Mean torque T_{mean}			100%	101%
Torque ripple $(T_{\max} - T_{\min})/T_{\mathrm{mean}}$			4.03%	2.96%
Max. total SPL L_p (dB(A))			69.13	50.25

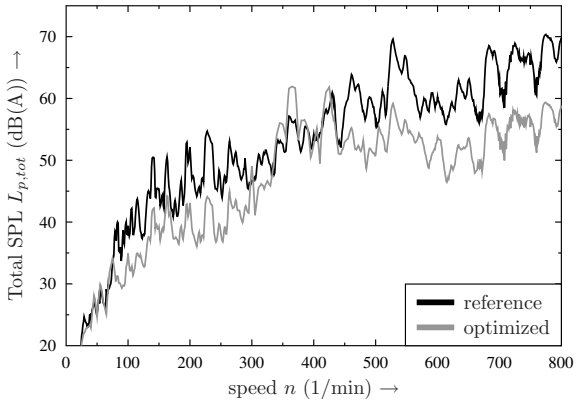

Figure 8. Simulated sound power level, comparison reference and optimized design.

The simulated A-weighted SPL obtained from the hybrid model and the FEM-to-measurement transfer function for both geometries is compared in Fig. 8. It shows that high values of total sound pressure at high speeds (reference geometry) are traded for comparatively higher values in the interval of 300 to 400 Hz, but still leading to the reduction of approx. 18dB(A). There is a slight difference between maximum SPL from the hybrid model and from FEM. However, the difference is not significant, since the tendency between optimized and reference geometry matches.

D. Verification by means of FEM

As additional verification of the proposed design, both designs are simulated using FEM in rated load condition. A comparison is given in Fig. 9. It can be seen, that even at rated load the proposed design should be significantly quieter.

IV. SUMMARY AND DISCUSSION

This paper proposes a methodology for the acoustic optimization of PMSM using two steps: hybrid modeling to obtain the magnetic field and forces and FEM-to-measurement transfer functions to assess the structural behavior and the radiation characteristics of the machine at once. Both steps have been discussed and are applied to a specific PMSM design, which is subject to optimization. The resulting optimized geometry shows significant reduction potential in terms of total SPL, up to 18dB(A), however at the cost of a larger magnet volume.

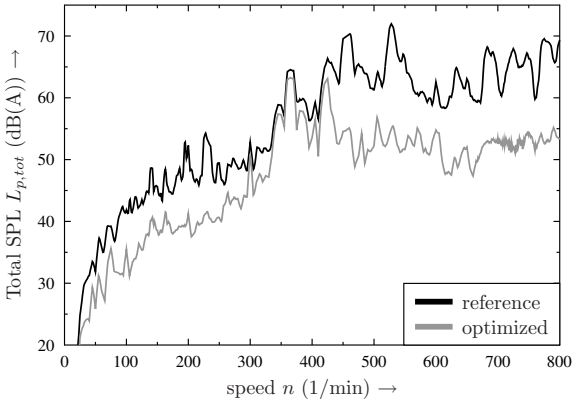

Figure 9. Full FEM simulation, comparison for full load.

As the proposed method relies on a given prototype of a similar machine, only those mode excited by this machine can be assessed and evaluated by means of transfer functions. Therefore, the change of pole-pair number or slot number. which may lead to different excited modes, need to be handled with care. As the approach lacks exactness due to various reasons, the value of potential reduction, 18dB(A) in this case, can only be considered a rough estimate. Nevertheless, a significantly quieter behavior is expected from the prototype featuring the proposed rotor geometry. This prototype is currently under construction. For more exact optimization results, it is always possible to employ FEM for the structural problem and BEM for the radiation phenomena, or perform a experimental modal analyses and treat vibration and radiation separately. Other combinations are possible to obtain transfer functions.

REFERENCES

[1] J. Fischer-Hinnen, "Über das Pfeifen von Maschinen," *Zeitschrift für Elektrotechnik*, vol. 23, p. 399, 1904.

[2] H. Frohne, "Über die primären Bestimmungsgrößen der Lautstärke bei Asynchronmaschinen," Ph.D. dissertation, Technische Universität Hannover, 1959.

[3] K. Delaere, W. Heylen, R. Belmans, and K. Hameyer, "Comparison of induction machine stator vibration spectra induced by reluctance forces and magnetostriction," *IEEE Transactions on Magnetics*, vol. 38, no. 2, pp. 969–972, 2002.

[4] H. Jordan, *Geräuscharme Elektromotoren*. W. Girardet, November 1950.

[5] G. Henneberger, P. Sattler, W. Hadrys, and D. Shen, "Procedure for the numerical computation of mechanical vibrations in electrical machines," *IEEE Transactions on Magnetics*, vol. 28, no. 2, pp. 1351–1354, March 1992.

[6] C. Neves, R. Carlson, N. Sadowski, J. Bastos, N. Soeiro, and S. Gerges, "Calculation of electromagnetic-mechanic-acoustic behavior of a switched reluctance motor," *IEEE Transactions on Magnetics*, vol. 36, no. 4, pp. 1364–1367, 2000.

[7] M. Furlan, A. Cernigoj, and M. Boltezar, "A coupled electromagnetic-mechanical-acoustic model of a DC electric motor," *COMPEL: The International Journal for Computation and Mathematics in Electrical and Electronic Engineering*, vol. 22, no. 4, pp. 1155–1165, 2003.

[8] C. Wang, J. Lai, and A. Astfalck, "Sound power radiated from an inverter driven induction motor II: Numerical analysis," *IEE Proceedings Electric Power Applications*, vol. 151, pp. 341–348, May. 2004.

[9] G. Jang and D. Lieu, "The effect of magnet geometry on electric motor vibration," *IEEE Transactions on Magnetics*, vol. 27, no. 6, pp. 5202 –5204, November 1991.

[10] K.-J. Han, H.-S. Cho, D.-H. Cho, and H.-K. Jung, "Optimal core shape design for cogging torque reduction of brushless dc motor using genetic algorithm," *IEEE Transactions on Magnetics*, vol. 36, no. 4, pp. 1927–1931, 2000.

[11] Y. Asano, Y. Honda, H. Murakami, Y. Takeda, and S. Morimoto, "Novel noise improvement technique for a PMSM with concentrated winding," in *Proceedings of the Power Conversion Conference, PCC Osaka 2002*, vol. 2, 2002, pp. 460–465 Vol.2.

[12] S.-I. Kim, J.-Y. Lee, Y.-K. Kim, J.-P. Hong, and Y.-H. Jung, "Optimization for reduction of torque ripple in interior permanent magnet motor by using the Taguchi method," *IEEE Transactions on Magnetics*, vol. 41, no. 5, pp. 1796 –1799, May 2005.

[13] G.-H. Kang, J. Hur, W.-B. Kim, and B.-K. Lee, "The shape design of interior type permanent magnet BLDC motor for minimization of mechanical vibration," in *Energy Conversion Congress and Exposition, ECCE 2009. IEEE*, September 2009, pp. 2409 –2414.

[14] S. Vivier, M. Hecquet, A. Ait-Hammouda, and P. Brochet, "Experimental design method applied to a multiphysical model trellis designs for a multidimensional screening study," *COMPEL: The International Journal for Computation and Mathematics in Electrical and Electronic Engineering*, vol. 24, no. 3, pp. 726–739, 2005.

[15] J. Roivainen, "Unit-wave response-based modeling of electromechanical noise and vibration of electrical machines," Ph.D. dissertation, Helsinki University of Technology, 2009.

[16] M. van der Giet, R. Rothe, M. Herranz Gracia, and K. Hameyer, "Analysis of noise exciting magnetic force waves by means of numerical simulation and a space vector definition," in *18th International Conference on Electrical Machines, ICEM 2008*, Vilamoura, Portugal, September 2008.

[17] D. Zarko, D. Ban, and T. Lipo, "Analytical calculation of magnetic field distribution in the slotted air gap of a surface permanent-magnet motor using complex relative air- gap permeance," *IEEE Transactions on Magnetics*, vol. 42, no. 7, pp. 1828–1837, 2006.

[18] M. Hafner, D. Franck, and K. Hameyer, "Static electromagnetic field computation by conformal mapping in permanent magnet synchronous machines," *IEEE Transactions on Magnetics*, 2010.

[19] *VACOMAX VACODYM*, Vacuumschmelze, P.O. Box 2253 Grüner Weg 37 D 63412 Hanau/ Germany. [Online]. Available: www.vacuumschmelze.com

V. BIOGRAPHIES

Michael van der Giet was born in 1977 in Krefeld. He received his Dipl.-Ing. (MSc) degree in electrical engineering in 2004 from the Faculty of Electrical Engineering and Information Technology at RWTH Aachen University. Since, 2004 he has worked as a researcher at the "Institute of Electrical Machines" (IEM) at RWTH Aachen University. He is currently working towards his Ph.D. degree in the area of noise and vibration of electrical machines. In 2008, he became chief engineer at the IEM.

David Franck received his diploma in Electrical Engineering in 2008 as Engineer from the Faculty of Electrical Engineering and Information Technology at RWTH Aachen University. Since, 2008 he has worked as a researcher at the Institute of Electrical Machines (IEM) at RWTH Aachen University. He is currently working towards his doctoral degree in the area of noise and vibration of electrical machines.

Richard Rothe received his Dipl.-Ing. degree in electrical engineering in 2007 as Engineer from the Faculty of Electrical Engineering and Information Technology at the RWTH Aachen University. Since 2007 he has worked as a researcher at the "Institute of Electrical Machines" (IEM) at the RWTH Aachen University. He is currently working towards his Ph.D. degree and his current research interest are the numerical field simulation, diagnostics and lifetime apects of electrical machines.

Kay Hameyer received the M.Sc. degree in electrical engineering from the University of Hannover, Germany. He received the Ph.D. degree from University of Technology Berlin, Germany. In 2004 Dr. Hameyer was awarded his Dr. habil. from the faculty of Electrical Engineering of the Technical University of Poznan, Poland and was awarded the title of Dr. h.c. from the faculty of Electrical Engineering of the Technical University of Cluj Napoca, Romania. Until February 2004, Dr. Hameyer was a full professor with the K.U.Leuven in Belgium. Currently Dr. Hameyer is the director of the Institute of Electrical Machines at RWTH Aachen University, Germany. His research interests are numerical field computation, the design and control of electrical machines, and numerical optimisation strategies. Dr. Hameyer is an elected member of the board of the International Compumag Society, and a founding member of the executive team of the IET Professional Network Electromagnetics.